

Angular filtering by volume Bragg grating in photothermorefractive glass for nanosecond laser pulse

Baoxing Xiong (熊宝星)^{1,2,3}, Fan Gao (高帆)^{1,2,3}, Xiang Zhang (张翔)^{1,2,3,*},
and Xiao Yuan (袁孝)^{1,2,3}

¹School of Optoelectronic Science and Engineering, Soochow University, Suzhou 215006, China

²Jiangsu Provincial Key Laboratory of Advanced Optical Manufacturing Technologies and Key Laboratory of Modern Optical Technologies of the Ministry of Education, Suzhou 215006, China

³Collaborative Innovation Center of Suzhou Nano Science and Technology, Soochow University, Suzhou 215006, China

*Corresponding author: zxiang@suda.edu.cn

Received November 9, 2018; accepted January 15, 2019; posted online April 1, 2019

The two-dimensional angular filter based on volume Bragg gratings in photothermorefractive glass for a nanosecond (ns) laser pulse is demonstrated. The experimental results show that the near-field beam quality of the laser pulse was effectively improved. The near-field modulation and contrast ratio were improved by 1.75 and 4.48 times, respectively. The power spectral density curves showed that the spatial frequencies more than 0.9 mm^{-1} in the x direction and 1.2 mm^{-1} in the y direction were effectively suppressed.

OCIS codes: 050.7330, 090.7330.

doi: 10.3788/COL201917.040501.

The near-field uniformity of a laser beam was extremely limited by noise with the medium and high frequencies in the high-power laser system^[1–4]. The poor beam quality may directly lead to the small-scale self-focusing and cause the optical components damage, which greatly restricts the output ability of the laser system. The traditional pinhole spatial filtering based on the “4f” system can improve the near-field uniformity, effectively control the rapid nonlinear growth, and ensure the safe operation of the laser system^[5]. However, the spatial filter generally requires a high-vacuum chamber to eliminate the breakdown at the focus. Moreover, this filter also requires a huge space to eliminate the spherical aberration and avoid pinhole closure^[6–10]. In order to solve the above problems, the angular filtering based on volume Bragg gratings (VBGs) was proposed^[11]. Since this new-type filter has great angular selectivity, it can control the medium and high spatial frequencies in the laser beam and directly improve its near-field uniformity, which can also effectively reduce the scale and cost of the laser system. In 1989, the Bragg gratings in photorefractive germanosilicate fibers were proposed by Meltz *et al.*^[12]. In the 1990s, the electrically switchable volume gratings in polymer-dispersed liquid crystals (PDLCs) were reported by Sutherland *et al.*^[13], and the volume structure was confirmed with scanning electron microscopy (SEM). The non-spatial filter based on volume holographic gratings recorded in different photosensitive materials was proposed by Ludman *et al.*^[14–16]. The design and preparation method of this grating were studied, and the angular selectivity of these gratings was demonstrated with a divergence beam. In 2009, the experiment on the low-pass non-spatial filter based on VBGs recorded in a photopolymer was demonstrated by Zheng *et al.*^[17]. In 2011, Zheng *et al.* reported the experiment on one-dimensional spatial filtering with the transmitting

VBGs^[18]. Then, Zhang *et al.* discussed low-pass spatial filters based on multilayer dielectric film and validated their filtering performance in 2014^[19]. However, the low laser damage threshold of the above materials limits their application in high-power laser fields. In the 1990s, the photothermorefractive (PTR) glass developed by Glebov *et al.* was used to record VBGs^[20,21]. Its good thermal stability and damage threshold make it possible to apply in the high-power laser fields^[22]. In our previous research, the angular filtering based on VBGs recorded in PTR glass was proposed and performed. The near-field uniformity and wavefront distribution of the laser beam were both remarkably improved^[11,23]. The diffraction characteristics of VBGs under high-flux laser irradiation were also discussed^[24]. Additionally, the hybrid filter^[25] and non-sidelobe angular filter^[26] were proposed to further optimize the non-spatial filter. However, the laser beam used in these researches was always the continuous wave (CW). Recently, Anderson *et al.* proposed to suppress the higher-order transverse modes of the Q -switched laser by using transmitting Bragg gratings (TBGs) as intra-cavity angular filters^[27]. But, the angular filter for spatial filtering in the near-field based on VBGs has not been reported.

In this Letter, the experiment on a two-dimensional (2D) angular filter based on VBGs in PTR glass for nanosecond (ns) laser pulse transmitting is demonstrated. The near-field modulation (M) and contrast (C) ratio were used to evaluate the output beam quality of the angular filter. The characteristics of the spatial filter were evaluated with power spectral density (PSD).

The schematic diagram of the experiment on an angular filter for a ns laser pulse is shown as Fig. 1(a). The laser beam used in this experiment was a pulse laser with the central wavelength of 1053 nm, the output energy of 140 mJ, and the pulse duration of 3 ns. The flat-topped

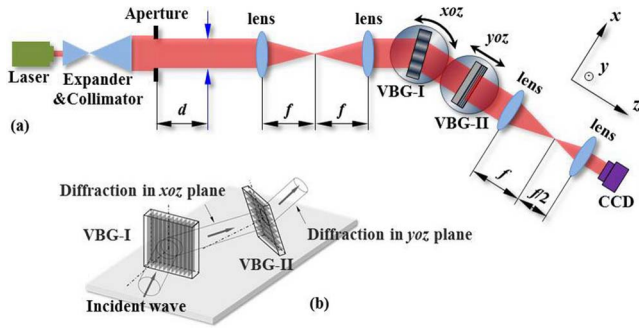


Fig. 1. (a) Schematic diagram of the experiment on an angular filter for an ns pulse laser. (b) The structural schematic diagram of a 2D angular filter.

beam with the size of $10 \text{ mm} \times 10 \text{ mm}$ was obtained with a combination of the expander, the collimator, and the hard-edged aperture. It turned into the modulated beam after propagating about $d = 0.5 \text{ m}$. Then, the modulated beam passed through the first image relay system with the focal length of 500 mm and was incident on the 2D angular filter at the Bragg angle. The 2D angular filter in the experiment consisted of two transmitting VBGs. The distance between two VBGs was only 30 mm . As shown in Fig. 1(b), VBG-I with vertical grooves was used to eliminate the modulation in the horizontal direction, and VBG-II with horizontal grooves was used to eliminate the modulation in the vertical direction. To avoid the diffraction effect, the filtered beam passed through the second image relay system with the focal lengths of 500 and 250 mm . Finally, the CCD was used to record the beam profile of the filtered beam.

The Bragg selectivity of transmitting VBGs can be described as Eq. (1)–(3), according to the coupled-wave theory^[28], where Δn is the refractive index modulation, d is the grating thickness, Λ is the grating period, ϕ is the slanted angle of the grating vector, n_0 is the average refractive index of the grating, λ is the wavelength of the incident beam, θ_0 is the Bragg angle inside the grating, and θ_r and θ_s are the angles of the incident and diffracted beams, respectively. $\Delta\theta$ and $\Delta\lambda$ are the deviation angle and wavelength from the Bragg condition, respectively:

$$\eta = \frac{\sin^2 \sqrt{\nu^2 + \xi^2}}{1 + \xi^2/\nu^2}, \quad (1)$$

$$\nu = \frac{\pi \Delta n d}{\lambda \sqrt{\cos \theta_r \cos \theta_s}}, \quad (2)$$

$$\xi = \frac{\pi \Delta \theta \sin(\phi - \theta_0) d}{\Lambda \cos \theta_s} = -\frac{\pi \Delta \lambda d}{2n_0 \Lambda^2 \cos \theta_s}. \quad (3)$$

Relevant structural parameters of two VBGs were shown in Table 1. The peak diffraction efficiencies of two VBGs were 96.5% and 97.7% , respectively. The damage thresholds were above 10 J/cm^2 . The angular selectivity was stimulated, as shown in Fig. 2. The angular selectivities of two VBGs (half-width at the first zero

Table 1. Parameters of the VBGs Used in the Experiment

	VBG-I	VBG-II
Central wavelength	1053 nm	
Period	$2.50 \mu\text{m}$	$3.49 \mu\text{m}$
Thickness	3.54 mm	
Tilt angle	-0.16°	0.14°
Bragg angle	11.9°	8.9°

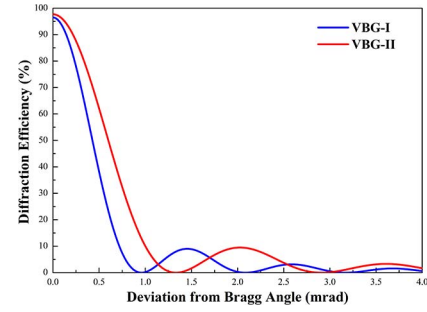


Fig. 2. Stimulated angular selectivity of two VBGs.

point, HWFZ) were about 0.96 and 1.30 mrad , respectively. The spectral selectivities of two VBGs (HWFZ) were both more than 4.5 nm .

The near-field distributions of the modulated beam and filtered beam through the 2D angular filter are shown in Fig. 3. Abundant spatial modulations, such as the square Fresnel diffraction rings, were introduced in the modulated beam by the hard aperture. After the two VBGs, the Fresnel diffraction rings were remarkably eliminated.

Generally, the near-field M and C ^[29] were used to evaluate the near-field beam quality, which were defined as

$$M = I_{\max}/I_{\text{avg}}, \quad (4)$$

$$C = \frac{1}{I_{\text{avg}}} \sqrt{\sum_{i=1}^N (I_i - I_{\text{avg}})^2 / N}, \quad (5)$$

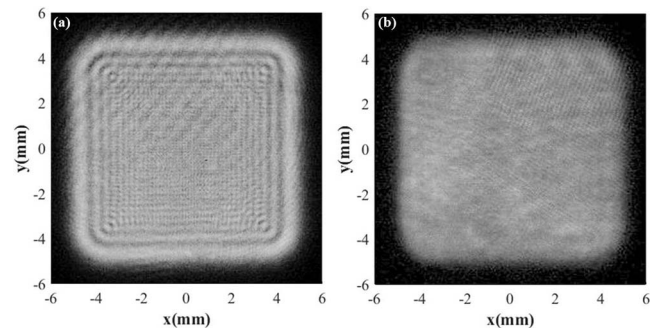


Fig. 3. Near-field distribution of the (a) modulated beam and (b) filtered beam through the angular filter.

where N is the number of sampling points, I_i is the intensity corresponding to the i th point, and I_{avg} is the average intensity of the all N points. The near-field modulation, which is defined as the ratio between the maximum peak intensity and the average intensity in the beam flat-top region, reflects directly the near-field intensity fluctuations. The near-field contrast ratio reflects the root mean square (RMS) of the intensity fluctuation in the near-field. The corresponding near-field M and C of the modulated and filtered beams were given in Table 2. The M and C were improved by 1.75 and 4.48 times after the 2D angular filter based on VBGs, respectively.

The PSD, as an analytical method in the spatial frequency domain, can quantitatively describe the relative distribution of each spatial frequency^[30]. Figure 4 shows the PSD of the modulated and filtered beams in the x and y directions, respectively. The spatial frequencies greater than 0.60 mm^{-1} were introduced into the laser beam with the hard aperture, as shown by the black line

Table 2. Results of M and C

	Modulated Beam	Filtered Beam
M	1.954	1.115
C	38.5%	8.6%

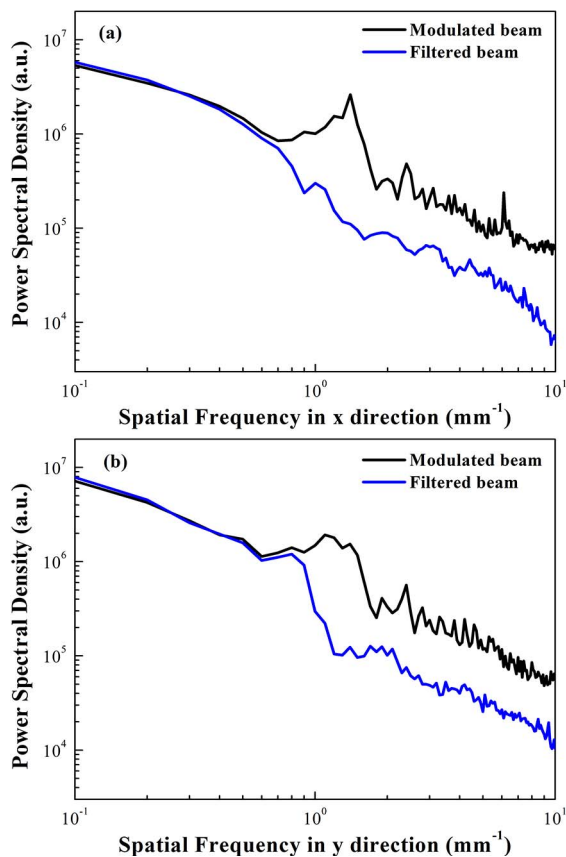


Fig. 4. PSD curves of the modulated and filtered beams in (a) the x direction and (b) the y direction.

in Fig. 4. After filtered with the 2D angular filter based on VBGs, the spatial frequencies more than 0.9 mm^{-1} in the x direction and 1.2 mm^{-1} in the y direction were remarkably suppressed, as shown by the blue line in Fig. 4.

In this experiment, since the spectral selectivity of two VBGs was larger than the spectral width of the laser pulse, the 2D angular filter almost had no effect on the spectral distribution and temporal profile of the laser pulse.

In summary, the 2D angular filter based on VBGs for a ns laser pulse is demonstrated and characterized with the near-field modulation, contrast ratio, and PSD. The near-field beam quality has been improved remarkably. The near-field modulation and contrast ratio were improved by 1.75 and 4.48 times, respectively. The spatial frequencies more than 0.9 mm^{-1} in the x direction and 1.2 mm^{-1} in the y direction were effectively suppressed. This method has potential applications in high-power laser pulse systems.

This work is supported by the National Key R&D Program of China (No. 2016YFF0100900), the National Natural Science Foundation of China (NSFC) (Nos. 61775153, 61705153, and 11504255), the Natural Science Foundation of Jiangsu Province (No. BK20141232), and the Priority Academic Program Development of Jiangsu Higher Education Institutions (PAPD).

References

1. A. E. Erlandson, K. S. Jancaitis, G. Letouze, C. D. Mashall, S. E. Seznec, and L. E. Zapata, Proc. SPIE **3492**, 638 (1999).
2. W. H. Williams, J. M. Auerbach, M. A. Hensian, and J. K. Lawson, Proc. SPIE **3264**, 93 (1998).
3. D. M. Aikens, C. R. Wolfe, and J. K. Lawson, Proc. SPIE **2576**, 281 (1995).
4. A. M. Rubenchik, S. K. Turitsyn, and M. P. Fedoruk, Opt. Express **18**, 1380 (2010).
5. J. T. Hunt, J. A. Glaze, W. W. Simmons, and P. A. Renard, Appl. Opt. **17**, 2053 (1978).
6. J. S. Pearlman and J. P. Anthes, Appl. Opt. **16**, 2328 (1977).
7. J. E. Murray, D. Milam, C. D. Boley, K. G. Estabrook, and J. A. Caird, Appl. Opt. **39**, 1405 (2000).
8. S. A. Dimakov, S. I. Zavgorodnaya, L. V. Koval'chuk, A. Y. Rodionov, and V. P. Yashukov, Sov. J. Quantum Electron. **19**, 803 (1989).
9. J. M. Auerbach, N. C. Holmes, J. T. Hunt, and G. J. Linford, Appl. Opt. **18**, 2495 (1979).
10. H. J. Zhang, S. L. Zhou, Y. E. Jiang, J. H. Li, W. Feng, and Z. Q. Lin, Chin. Opt. Lett. **10**, 060501 (2012).
11. X. Zhang, X. Yuan, S. Wu, J. S. Feng, K. S. Zou, and G. J. Zhang, Opt. Lett. **36**, 2167 (2011).
12. G. Meltz, W. W. Morey, and W. H. Glenn, Opt. Lett. **14**, 823 (1989).
13. R. L. Sutherland, V. P. Tondiglia, L. V. Natarajan, T. J. Bunning, and W. W. Adams, Appl. Phys. Lett. **64**, 1074 (1994).
14. J. E. Ludman, J. R. Riccobono, N. O. Reinhand, I. V. Semenova, Y. L. Korzinin, and M. S. Shahriar, Proc. SPIE **2532**, 481 (1995).
15. J. E. Ludman, J. R. Riccobono, N. O. Reinhand, I. V. Semenova, Y. L. Korzinin, M. S. Shahriar, H. J. Caulfield, J. M. Fournier, and P. Hemmer, Opt. Eng. **36**, 1700 (1997).
16. J. E. Ludman, J. R. Riccobono, N. O. Reinhand, Y. L. Korzinin, I. V. Semenova, and M. S. Shahriar, Quantum Electron. **26**, 1093 (1996).
17. H. B. Zheng, Y. L. He, J. C. Tan, G. W. Zheng, D. Y. Ding, X. Wang, and X. D. Wang, Proc. SPIE **7506**, 75062A (2009).

18. G. Zheng, B. Shen, J. Tan, Y. He, and X. Wang, *Chin. Opt. Lett.* **9**, 030501 (2011).
19. Y. Zhang, H. J. Qi, K. Yi, Y. Z. Wang, H. B. He, and J. D. Shao, *Chin. Opt. Lett.* **12**, S20501 (2014).
20. L. B. Glebov, N. V. Nikonorov, E. I. Panysheva, G. T. Petrovskii, V. V. Savvin, I. V. Tunimanova, and V. A. Tsekhomskii, *Sov. Phys. Dokl.* **35**, 878 (1990).
21. O. M. Efimov, L. B. Glebov, L. N. Glebova, K. C. Richardson, and V. I. Smirnov, *Appl. Opt.* **38**, 619 (1999).
22. O. M. Efimov, L. B. Glebov, S. Papernov, and A. W. Schmid, *Proc. SPIE* **3578**, 554 (1999).
23. F. Gao, X. Zhang, X. J. Sun, and X. Yuan, *Opt. Lett.* **41**, 1082 (2016).
24. X. Zhang, J. S. Feng, B. X. Xiong, K. S. Zou, and X. Yuan, *Opt. Express* **22**, 8291 (2014).
25. X. Zhang, X. Yuan, J. S. Feng, F. Gao, B. X. Xiong, and K. S. Zou, *Opt. Lett.* **39**, 663 (2014).
26. F. Gao, X. Yuan, and X. Zhang, *Chin. Opt. Lett.* **14**, 060502 (2016).
27. B. M. Anderson, E. Hale, G. Venus, D. Ott, I. Divliansky, and L. Glebov, *Proc. SPIE* **9726**, 972611 (2016).
28. H. Kogelnik, *Bell Syst. Tech. J.* **48**, 2909 (1969).
29. Z. H. Sun, Z. T. Peng, H. Liu, L. B. Xu, J. P. Zhao, C. Wang, and X. J. Fu, *Chin. J. Lasers* **35**, 544 (2008).
30. J. M. Elson and J. M. Bennett, *Appl. Opt.* **34**, 201 (1995).